20/30 GHz dual-band circularly polarized reflectarray antenna based on the concentric dual split-loop element

Smith, Thomas Gunst; Vesterdal Larsen, Niels; Vesterager Gothelf, Ulrich; Kim, Oleksiy S.; Breinbjerg, Olav

Published in:
Proceedings of 34th ESA Antenna Workshop

Publication date:
2012

20/30 GHZ DUAL-BAND CIRCULARLY POLARIZED REFLECTARRAY ANTENNA BASED ON THE CONCENTRIC DUAL SPLIT-LOOP ELEMENT

Thomas Gunst Smith[1,2], Niels Vesterdal Larsen[1], Ulrich Vesterager Gothelf[1], Oleksiy S. Kim[2], and Olav Breinbjerg[2]

[1]*Thrane & Thrane A/S, Lundtoftegårdsvej 93D, DK-2800 Kgs. Lyngby, Denmark*
[2]*Department of Electrical Engineering, Electromagnetic Systems, Technical University of Denmark, Ørsteds Plads, Building 348, DK-2800 Kgs. Lyngby, Denmark*

ABSTRACT

A concentric dual split-loop element is designed and investigated for reflectarray antenna design in the emerging 20 GHz and 30 GHz Ka-band satellite communication spectrum. The element is capable of providing adjustment of the phase of reflection coefficients for circular plane waves in two separate frequency bands, by rotation of the individual split-loops. Cross-polar reflection is simultaneously minimized by optimizing the gaps in the split-loops. Based on the element characteristics, an iterative design procedure is proposed and used to design a front-fed reflectarray antenna. The aperture efficiency exceeds 56 % with an on-axis axial ratio below 0.21 dB in both frequency bands.

1. INTRODUCTION

A reflectarray antenna generally consists of an array of scattering elements and a feeding antenna. The operating principle is derived from classical reflector antennas, where a shaped surface can be designed to produce e.g. a pencil or contoured beam. However, for planar reflectarrays, the scattering elements are designed to reflect the incident field with a desired phase, such that a given farfield can be achieved [1].

For high-gain antennas, printed reflectarrays are of particular interest due to their low cost, ease of manufacture and reconfigurability [2]. Thus a printed reflectarray is a feasible candidate for user terminal antennas for satellite communication in the emerging Ka-band spectrum. When choosing the reflectarray element topology, the requirements to polarization and bandwidth are essential. For circular polarization, commonly used elements include stub-tuned patches [3], crossed dipoles [4, 5] and single split-loops [6, 7]. However, for large reflectarrays the differential spatial phase delay is significant [8] making it extremely challenging to cover the entire $20 - 30$ GHz frequency band, thus it is preferred to utilize a reflectarray element which allows separate phase adjustment in the 20 and 30 GHz frequency bands. For this purpose, a concentric dual split-loop element utilizing the element rotation technique is proposed. The element is investigated and optimized for dual-frequency circular polarization, specifically LHCP from 19.7 to 20.2 GHz (RX) and RHCP from 29.5 to 30.0 GHz (TX). This element was suggested in [1, p. 122], but to the best of our knowledge it has not been subject to detailed investigations.

2. ELEMENT DESIGN AND INVESTIGATION

The commercially available software Ansoft Designer has been employed to optimize the element geometry. By using periodic boundary conditions and plane wave excitation the element is simulated as if it was located in a two dimensional infinite square grid array, with an inter-element spacing of 5 mm. The element has shown stable performance over relevant incidence angles; hence only normal incidence is considered in this paper.

2.1. Element Rotation Technique

A local (u, v) coordinate system is assigned to the element under consideration, which in Figure 1 is exemplified by a simple dipole though the following is valid for arbitrary element geometries. The rotation of the local coordinate system, and thus the element, can be described in the global (x, y) coordinate system by the rotation angle ψ.

An incident RHCP plane wave is considered traveling in the negative z-direction $\boldsymbol{E}^{\mathrm{i}} = (\hat{x} + j\hat{y})\, E_0 e^{jkz}$, where E_0 is the electric field amplitude and k is the free-space

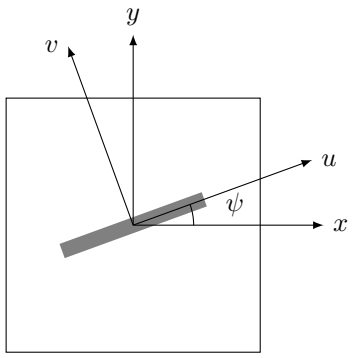

Figure 1. Global (x, y) and local (u, v) coordinate system for element rotation.

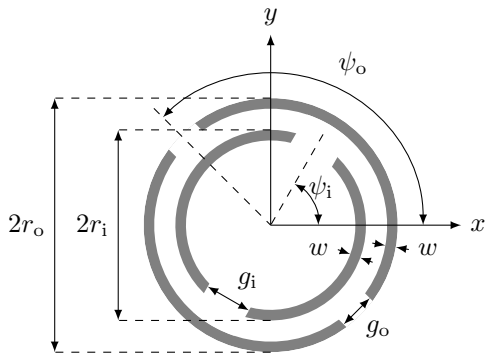

Figure 2. Concentric dual split-loop reflectarray element geometry.

wavenumber. The time-factor $e^{j\omega t}$ is assumed and suppressed. By decomposing this incident field along the u- and v-directions and employing the associated linear reflection coefficients, R_u and R_v, it can readily be shown that the reflected far-field plane wave can be described by

$$\begin{aligned} \boldsymbol{E}^{\mathrm{s}} &= \frac{1}{2}\Bigg(\left(R_u - R_v\right)\left[\hat{x} - j\hat{y}\right] e^{j2\psi} \\ &\quad + \left(R_u + R_v\right)\left(\hat{x} + j\hat{y}\right)\Bigg] E_0 e^{-jkz}, \end{aligned} \tag{1}$$

where R_u, R_v are the reflection coefficients of the linear electric field components along $\hat{u}, \hat{v}$, respectively. It is evident that for $R_u = R_v e^{j\pi}$, the scattered field is a pure RHCP plane wave traveling in the positive z direction and the phase scales linearly in ψ. However, if either $|R_u| \neq |R_v|$, or if the phase difference is not equal to π, cross-polarization (here LHCP) is introduced.

It is important to note that for elements placed in a reflectarray element grid, the coupling to the neighboring elements will generally change when the element is rotated. It is therefore crucial to modify the element geometry accordingly to keep $R_u = R_v e^{j\pi}$, such that the cross-polar reflection is suppressed [7]. This is usually achieved by an anisotropic design where only one of the two linear orthogonal polarizations excites a resonant element, e.g. a dipole on a grounded dielectric, as depicted in Figure 1. In the case of resonance, the polarization parallel to the dipole will see a reflection with zero phase, whereas the orthogonal polarization will be reflected with a phase equal to π due to the infinite ground-plane. Therefore, if the dipole length is adjusted properly, a phase-difference of π is ensured. However, since the losses increase significantly around the resonance, the amplitude of the parallel component will be smaller than the orthogonal. It is thus clear that the losses put a constraint on the cross-polarization level that can be achieved.

2.2. Concentric Dual Split-Loop Element

The concentric dual split-loop element proposed in this paper is illustrated in Figure 2. The outer and inner split-loop is characterized by the radii r_{o} and r_{i}, respectively, measured from the center to the outside of the conductor, the rotation angles ψ_{o} and ψ_{i}, the gap sizes g_{o} and g_{i}, and equal conductor width w. The element is printed on a grounded Rogers RT/Duroid 5880 substrate with dielectric constant $\epsilon_{\mathrm{r}} = 2.20$, dissipation factor $\tan\delta = 0.0009$ and thickness of $1.016\,\mathrm{mm}$.

The concept of the concentric dual split-loop element is that the inner and outer split-loop can be rotated such that desired reflection phases are obtained at 20 and 30 GHz simultaneously. As noted in Section 2.1, the geometry of the concentric dual split-loop element must be adjusted such that the orthogonal reflection coefficients have a phase difference of π, so that no cross-polarization occurs. However, when the outer and inner split-loops are rotated their coupling to each other and to neighboring elements change. Therefore, by adjusting the gaps of the split-loops, g_{o} and g_{i}, each element is optimized to minimize cross-polar reflection, for all rotation angles. In this way, the cross-polar reflection coefficient at both 20 and 30 GHz is suppressed below $-31\,\mathrm{dB}$ for all rotation angles. The optimized element geometry is given in Table 1. Due to the symmetry of the concentric dual split-loop element, all properties are 180° periodic in rotation, hence results are shown for ψ_{o} and ψ_{i} in the interval 0° to 180°.

Table 1. Reflectarray element geometry data.

r_{o}	$1.9\,\mathrm{mm}$
r_{i}	$1.4\,\mathrm{mm}$
w	$0.2\,\mathrm{mm}$
ψ_{o}, ψ_{i}	$[0^\circ; 180^\circ]$
g_{o}	$[0.46\,\mathrm{mm}; 0.52\,\mathrm{mm}]$
g_{i}	$[0.24\,\mathrm{mm}; 1.01\,\mathrm{mm}]$

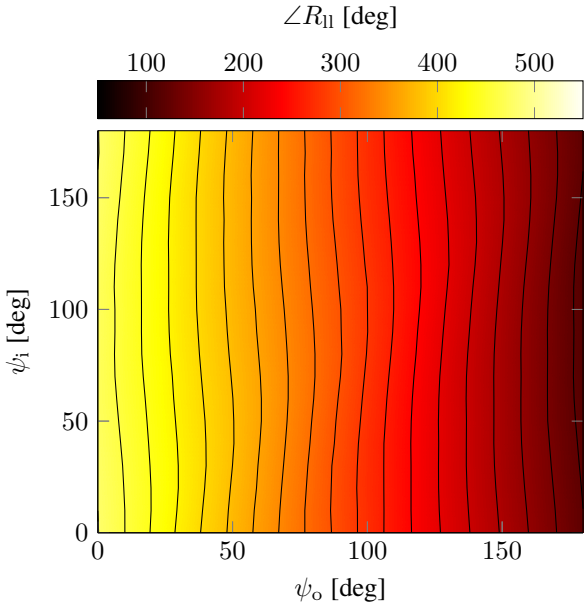

Figure 3. Phase of 20 GHz LHCP-to-LHCP reflection coefficient.

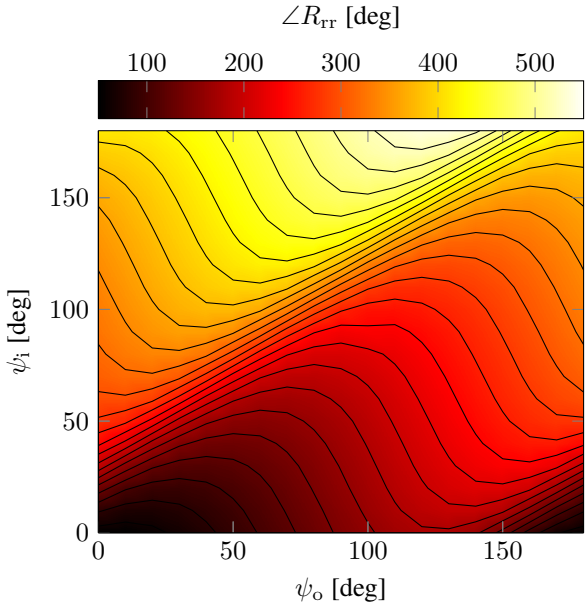

Figure 4. Phase of 30 GHz RHCP-to-RHCP reflection coefficient.

At 20 GHz, the reflection coefficient is primarily determined by ψ_{o} and almost unaffected by ψ_{i}, which can be seen in Figure 3, where $\angle R_{\mathrm{ll}}$ is the phase of the LHCP-to-LHCP circular reflection coefficient. The contour curves are almost vertical and equidistant, indicating that the rotation of the outer split-loop provides the desired linear phase adjustment over rotation angle ψ_{o} for any value of ψ_{i}. For a fixed value of ψ_{o}, the phase varies within $\pm 5.0^{\circ}$ when ψ_{i} is varied.

At 30 GHz, the reflection coefficients are found to depend on both ψ_{o} and ψ_{i}, which is evident in Figure 4, where $\angle R_{\mathrm{rr}}$ is the phase of the RHCP-to-RHCP reflection coefficient. However, an important feature is that for a fixed value of ψ_{o}, the phase is monotonic in ψ_{i}, which means that for a given rotation angle of the outer split-loop, there is a unique solution for the rotation angle of the inner split-loop which gives a desired reflection phase.

The phase range of the circular co-polar reflection coefficient is exactly 360°, for ψ_{o} or ψ_{i} in the interval 0° to 180°, at 20 and 30 GHz, respectively. This range is of course necessary for the use of the element in the reflectarray design. For all rotation angles of both the inner and outer split-loops, the amplitude of the co-polar reflection coefficient is above 0.26 and 0.35 dB over the entire RX and TX frequency bands, respectively.

The above mentioned characteristics of the circular reflection coefficients enables a design of a reflectarray antenna, where the reflectarray is first optimized for 20 GHz performance by determining ψ_{o} for all elements, and afterwards adjusting ψ_{i} for 30 GHz performance without affecting the radiation at 20 GHz significantly.

3. REFLECTARRAY DESIGN

Based on the element characteristics presented in Section 2, an iterative design procedure has been developed to determine ψ_{o} and ψ_{i} for each reflectarray element. In this section, the proposed design procedure is described and a concept reflectarray antenna design is presented.

3.1. Design Procedure

As stated in Section 2, the reflection coefficient at 20 GHz is almost unaffected by rotation of the inner split-loop, hence the reflectarray may be optimized for 20 GHz and subsequently 30 GHz. The reflectarray is designed for a single frequency in each of the two separate frequency bands, and the design procedure can generally be outlined as follows:

1. g_{o} and g_{i} are optimized for minimum cross-polar reflection using Ansoft Designer, for a finite set of ψ_{o} and ψ_{i}
2. ψ_{o} and ψ_{i} of all reflectarray elements are set to zero
3. ψ_{o} is determined for all reflectarray elements
   (a) A one dimensional 20 GHz phase-curve is generated for varying ψ_{o}, while keeping ψ_{i} fixed

(b) ψ_{o} is determined from the phase-curve and the desired reflected phase

4. ψ_{i} is determined for all reflectarray elements
   (a) A one dimensional 30 GHz phase-curve is generated for varying ψ_{i}, while keeping ψ_{o} fixed
   (b) ψ_{i} is determined from the phase-curve and the desired reflected phase
5. The scattered aperture field over the reflectarray is calculated
6. The radiated field of the entire reflectarray is calculated and the feed pattern is added

Step 3 and step 4 can be repeated such that the actual non-zero rotation angle of ψ_{i} is included when choosing ψ_{o}. This may be necessary for concentric dual split-loop geometries where the coupling between the two loops is larger at 20 GHz. However, for the present design a single iteration is sufficient.

The procedure has been implemented in a numerical code that calculates the radiated far-field by the equivalent currents technique [9, technique II].

3.2. Concept Design

To validate the proposed reflectarray element, a front-fed circular aperture reflectarray has been designed. The reflectarray is designed to have a broadside pencil beam towards $\theta = 0^\circ$ and consists of approximately $11,300$ elements. The developed code allows for an arbitrary feed antenna, but here a Gaussian beam feed model is used. The specifications of the reflectarray and feed antenna are summarized in Table 2.

The rotation angles of the concentric dual split-loop elements are shown in Figure 5. Due to the rotational symmetry of the reflectarray only a cross-section from the center to the edge is shown, where element 61 and 120 are the element near the center and edge, respectively. It is found that the rotation angle of the outer split-loop scales linearly with the distance from the element to the feed antenna, which is due to the linear $2\psi_{\mathrm{o}}$ reflection phase behavior and independence of ψ_{i}, as discussed in Section 2. However, the rotation angle of the inner split-loop is highly aperiodic. This is caused by the complex behavior of the reflection phase, as also discussed in Section 2.

Table 2. Specifications of front-fed reflectarray antenna.

RX	$19.7\,\mathrm{GHz} - 20.2\,\mathrm{GHz}$ LHCP
TX	$29.5\,\mathrm{GHz} - 30.0\,\mathrm{GHz}$ RHCP
Diameter	$60\,\mathrm{cm}$
Focal length	$46\,\mathrm{cm}$
Edge taper	$-12\,\mathrm{dB}$

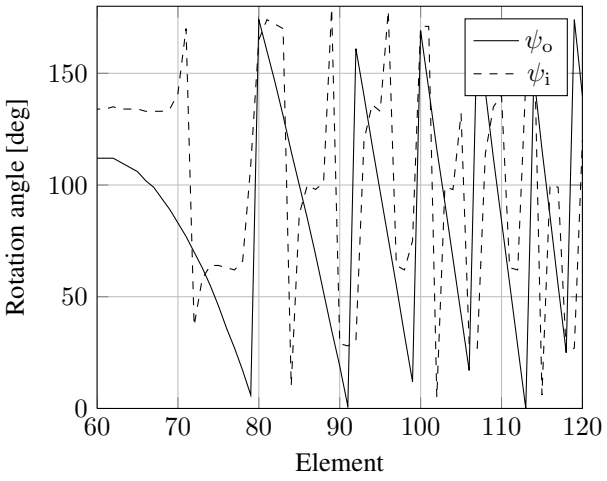

Figure 5. Rotation angles of reflectarray elements along radial cut from centre to edge of the circular aperture.

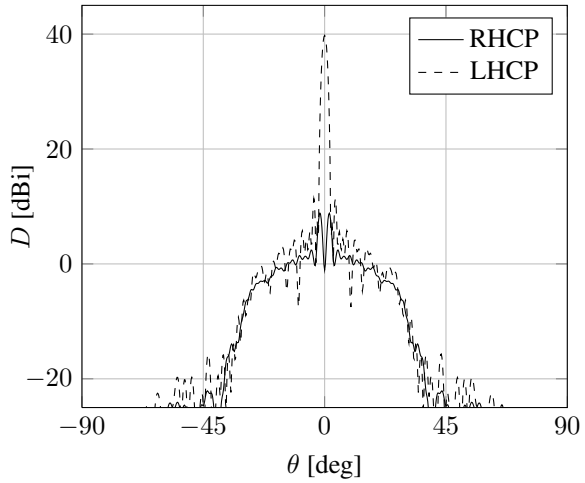

Figure 6. Radiation pattern of the designed reflectarray at 20 GHz.

The radiation pattern of the front-fed reflectarray is depicted in Figure 6 for 20 GHz and in Figure 7 for 30 GHz, with a zoom of the 30 GHz radiation pattern in Figure 8. At 20.0 GHz, the maximum directivity is 39.8 dBi, which corresponds to an aperture efficiency of 60 %, and the sidelobe level is 28.4 dB below peak. At 30.0 GHz, the maximum directivity is 43.2 dBi, which is an aperture efficiency of 58 %, and the sidelobe level is 30.4 dB below peak.

Over the RX and TX frequency bands, the on-axis co-polar directivity and axial ratio (AR) is plotted in Figure 9 and 10, respectively. The designed reflectarray antenna has an aperture efficiency exceeding 56 % and an on-axis AR below 0.21 dB over both the RX and TX frequency bands.

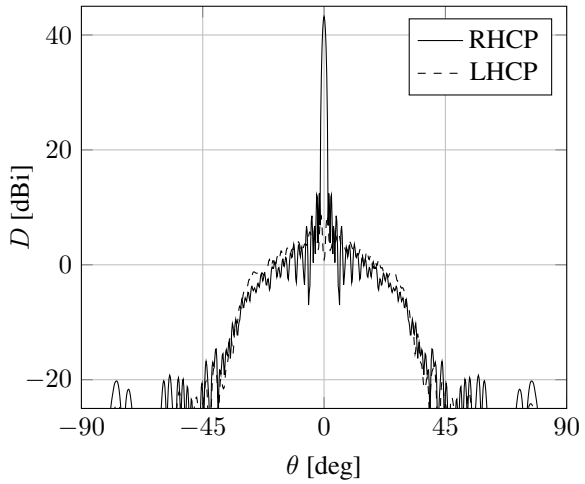

Figure 7. Radiation pattern of the designed reflectarray at 30 GHz.

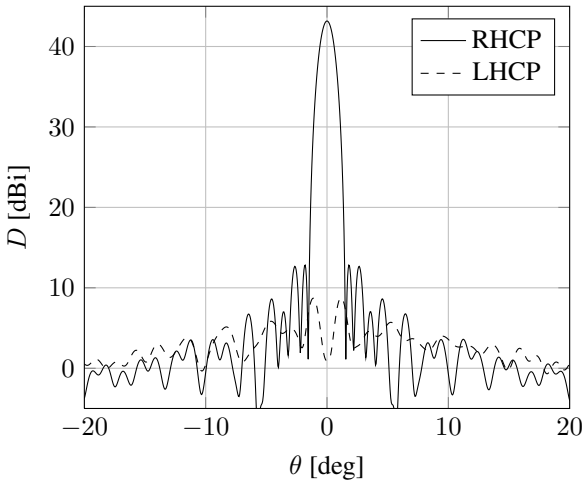

Figure 8. Zoom of the radiation pattern of the designed reflectarray at 30 GHz.

4. CONCLUSIONS

A concentric dual split-loop reflectarray element for dual-band circular polarization has been presented. The element provides means for adjusting the phase of circular reflection coefficients in two separate frequency bands. By optimizing the element geometry, the cross-polar reflection coefficient of the element has been suppressed below $-31\,\mathrm{dB}$ for all element rotation angles, at both design frequencies simultaneously.

An iterative design-procedure has been presented, and a front-fed reflectarray antenna has been designed for dual-band 20 and 30 GHz application. The reflectarray shows satisfying performance in both frequency bands, with an aperture efficiency above $56\,\%$ and on-axis AR below $0.21\,\mathrm{dB}$.

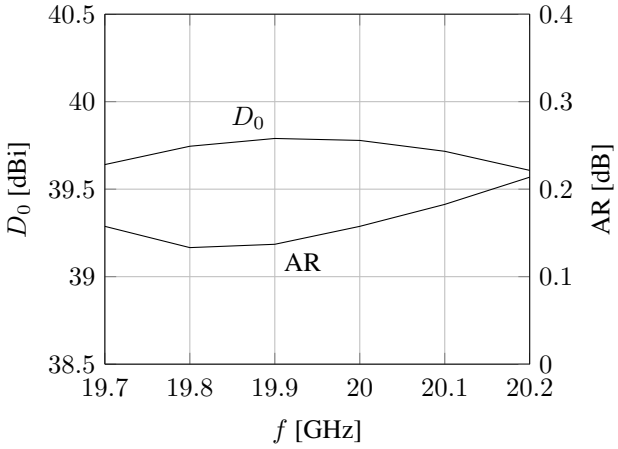

Figure 9. On-axis directivity and AR in RX frequency band.

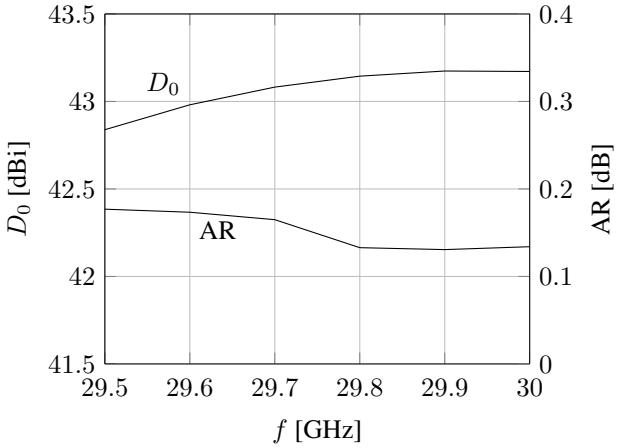

Figure 10. On-axis directivity and AR in TX frequency band.

A prototype reflectarray is planned to be manufactured and measured in the near future to validate the presented results.

REFERENCES

[1] J. Huang and J. A. Encinar. *Reflectarray Antennas*. IEEE Press, 2008.

[2] J. A. Encinar. Recent advances in reflectarray antennas. In *Proceedings of the European Conference on Antennas and Propagation*, pages 1–6, 2010.

[3] J. Huang and R. J. Pogorzelski. A Ka-band microstrip reflectarray with elements having variable rotation angles. *IEEE Transactions on Antennas and Propagation*, 46(5):650–656, 1998.

[4] E. B. Felstead, J. Shaker, M. R. Chaharmir, and A. Petosa. Enhancing multiple-aperture ka-band

navy SATCOM antennas with electronic tracking and reflectarrays. In *MILCOM 2002. Proceedings*, volume 2002 of *1*, pages 168–172. IEEE, October 2002.

[5] R. Chaharmir, J. Shaker, and M. Cuhaci. Development of dual-band circularly polarised reflectarray. In *IEE Proceedings - Microwaves, Antennas and Propagation*, volume 153, pages 49–54, 2006.

[6] B. Strassner, C. Han, and K. Chang. Circularly polarized reflectarray with microstrip ring elements having variable rotation angles. *IEEE Transactions on Antennas and Propagation*, 52(4):1122–1125, April 2004.

[7] A. Yu, F. Yang, A. Z. Elsherbeni, J. Huang, and Y. Kim. An offset-fed x-band reflectarray antenna using a modified element rotation technique. *IEEE Transactions on Antennas and Propagation*, 60(3):1619–1624, March 2012.

[8] D. M. Pozar. Bandwidth of reflectarrays. *Electronics Letters*, 39(21):1490–1491, 2003.

[9] M. Zhou, S. B. Sorensen, E. Jorgensen, P. Meincke, O. S. Kim, and O. Breinbjerg. An accurate technique for calculation of radiation from printed reflectarrays. *IEEE Antennas and Wireless Propagation Letters*, 10:1081–1084, 2011.